

# ANCHOR NODES REFINEMENT IN JOINT LOCALIZATION AND SYNCHRONIZATION OF A SENSOR NODE

Liyang Rui      Shanjie Chen      K. C. Ho

ECE Department, University of Missouri, Columbia, MO 65211, USA

## ABSTRACT

This paper proposes an estimator for refining the inaccurate positions and clocks of the anchors during the localization and synchronization of a sensor node in a wireless sensor network. It solves the highly nonlinear problem in closed-form through parameter transformation and multi-stage weighted least squares processing. Theoretical analysis and simulation studies show that the proposed estimator is able to provide the CRLB accuracy for both the sensor node and the anchors under reasonable amount of Gaussian errors.

**Index Terms**— Algebraic solution, localization, synchronization, wireless sensor network

## 1. INTRODUCTION

Precise localization of sensor nodes in a wireless sensor network (WSN) relies on range-based measurements, such as time of arrival (TOA) [1–3] or time difference of arrival (TDOA) [4–7], among the sensors and the anchors. Acquisition of the time information necessitates synchronization. Many protocols have been proposed over the years to synchronize the nodes, including the reference broadcast synchronization (RBS) [8], the flooding time synchronization protocol (FTSP) [9] and more recently the distributed Bayesian inference method [10]. Traditionally, the synchronization and localization problems have been handled separately. When considering and formulating synchronization as an estimation task, it is possible to combine the synchronization and localization problems and solve them together to improve performance.

Using successive message exchanges between a sensor node and the anchors and modeling the clock differences by drifts and offsets, [11–14] have shown the feasibility of joint localization and synchronization of a sensor node. The resulting problem, however, is highly nonlinear and challenging to solve. [12] derived an explicit solution by linearizing the time measurement equations with respect to the unknowns. [13] proposed an algebraic solution that is able to give the Cramer-Rao Lower Bound (CRLB) accuracy. The above studies [11–13] used an ideal condition that the positions of the anchors are exactly known and their clocks are perfectly synchronized. This condition is seldom satisfied in practice [10, 15–17], especially considering that the anchors could be previously located and synchronized sensor nodes. Simply pretending it is true would reduce performance [14, 18].

To account for the anchor position and clock uncertainties, [14] applied the generalized total least squares (GTLS) technique to obtain a sub-optimum position and synchronization solution for a single sensor node. Rui and Ho [18] extended the study for multiple sensor nodes and proposed a different algebraic solution that is able to attain the CRLB accuracy. These algorithms focus on the sensor nodes only and ignore any opportunity to refine the anchors. The anchor nodes could be used to locate and synchronize other sensors,

and they could also be previously estimated sensor nodes. It is important to improve the positions and synchronization of the anchors.

This paper proposes an estimator to perform joint localization and synchronization of a single sensor node and the refinement of those for the anchor nodes together. This is a highly nonlinear estimation problem and we solve it using parameter transformation and multi-stage processing. The proposed solution is algebraic, computationally attractive and able to reach the CRLB performance. Different from [19–21] that address either anchor position or clock uncertainties, we improve both the positions and synchronizations of the anchors jointly. In addition, the approach we take is separated from those in [14, 18], where we exploit not only the connections between the sensor node and the anchors, but also those among the anchors. The connections among the anchors improve their estimation, leading to better accuracy for the sensor node as well as improving the positioning and synchronization of subsequent sensor nodes in the network.

We shall use bold lower case letter to denote column vector and bold upper case letter to represent matrix. The symbols  $\mathbf{1}_p$ ,  $\mathbf{0}_p$  and  $\mathbf{1}_p^\perp$  designate length  $p$  column vectors of ones, zeros and alternating  $-1$  and  $1$ .  $\mathbf{I}_p$  is an identity matrix of size  $p$  and  $\mathbf{O}_{p \times q}$  is a  $p \times q$  zero matrix. The true value of an erroneous vector  $\mathbf{a}$  is  $\mathbf{a}^o$ .  $a(i)$  is the  $i$ -th element of  $\mathbf{a}$  and  $\mathbf{a}(i : j)$  is the subvector having the  $i$ -th to the  $j$ -th elements. The symbols  $\otimes$  and  $\odot$  represent the Kronecker product and the element by element multiplication.  $\text{diag}(+, \times, \dots)$  is a block diagonal matrix with blocks  $+$ ,  $\times$ ,  $\dots$ .

We present the problem in Section 2 and propose the solution in Section 3. Section 4 provides the analysis and Section 5 examines the performance by simulation. Section 6 is the conclusion.

## 2. PRELIMINARY

We are interested in using  $M$  anchor nodes at  $\mathbf{a}_i^o \in \mathbb{R}^K$  with clock drift  $\alpha_i^o$  and offset  $\beta_i^o$  to determine the location  $\mathbf{b}^o \in \mathbb{R}^K$  and clock parameters  $\alpha_b^o$  and  $\beta_b^o$  of a sensor node, where  $i = 1, 2, \dots, M$  and  $K$  is the dimension of localization. Anchor uncertainties are present and we only observe the noisy values  $\mathbf{a}_i = \mathbf{a}_i^o + \boldsymbol{\epsilon}_{\mathbf{a},i}$ ,  $\alpha_i = \alpha_i^o + \epsilon_{\alpha,i}$ ,  $\beta_i = \beta_i^o + \epsilon_{\beta,i}$ , where  $\boldsymbol{\epsilon}_{\mathbf{a},i}$ ,  $\epsilon_{\alpha,i}$  and  $\epsilon_{\beta,i}$  are additive noise. The anchor parameters are collectively represented by  $\boldsymbol{\theta}_{\mathbf{a}} = [\boldsymbol{\theta}_1^T, \boldsymbol{\theta}_2^T, \dots, \boldsymbol{\theta}_M^T]^T = \boldsymbol{\theta}_{\mathbf{a}}^o + \boldsymbol{\epsilon}_{\mathbf{a}}$ , where  $\boldsymbol{\theta}_i = [\mathbf{a}_i^T, \alpha_i, \beta_i]^T$ . We assume  $\boldsymbol{\epsilon}_{\mathbf{a}}$  is zero-mean Gaussian with covariance matrix  $\mathbf{Q}_{\mathbf{a}}$  [10, 17]. The unknown vector for the sensor node is denoted similarly as  $\boldsymbol{\theta}_b^o = [\mathbf{b}^{oT}, \alpha_b^o, \beta_b^o]^T$ . The total unknown vector to be found is  $\boldsymbol{\theta}^o = [\boldsymbol{\theta}_b^{oT}, \boldsymbol{\theta}_{\mathbf{a}}^{oT}]^T$ .

The measurements to obtain  $\boldsymbol{\theta}^o$  are the time stamps from two-way message exchanges [13, 14, 22–25] between the sensor node and an anchor. As shown in Fig. 1, the sensor node sends out the first message embedded with the sending time  $T_{i,1}$ , and anchor node  $i$  returns back the message. The sequential  $l$ -th replication con-

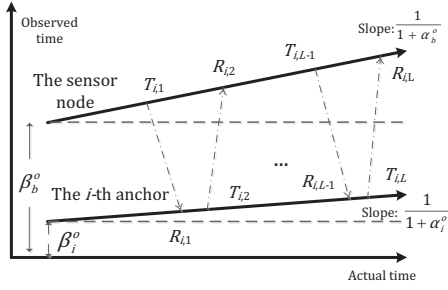


**Fig. 1.** The two-way message exchanges between the sensor node and the  $i$ -th anchor node.

tains the stamps of current sending time and the most recent receiving time,  $T_{i,l}$  and  $R_{i,l-1}$ . After  $L$  exchanges, we collect them as  $\mathbf{t}_i = [T_{i,1}, R_{i,2}, T_{i,3}, R_{i,4}, \dots, T_{i,L-1}, R_{i,L}]^T$  from the sensor and  $\mathbf{r}_i = [R_{i,1}, T_{i,2}, R_{i,3}, T_{i,4}, \dots, R_{i,L-1}, T_{i,L}]^T$  from the anchor. They are related to the unknowns  $\theta_i^o$  and  $\theta_b^o$  by [14, 18]

$$(\mathbf{t}_i - \mathbf{1}_L \beta_b^o)(1 + \alpha_b^o) = (\mathbf{r}_i - \mathbf{1}_L \beta_i^o)(1 + \alpha_i^o) + \mathbf{1}_L^{\perp} \|\mathbf{a}_i^o - \mathbf{b}^o\|/c + \mathbf{1}_L^{\perp} \odot \mathbf{n}_i \quad (1)$$

where  $c$  is the speed of light,  $\|\cdot\|$  is the Euclidean norm of  $\cdot$ ,  $\mathbf{n}_i$  is the measurement noise vector, and  $i = 1, 2, \dots, M$ . We assume the noise vector  $\mathbf{n} = [\mathbf{n}_1^T, \mathbf{n}_2^T, \dots, \mathbf{n}_M^T]^T$  is zero-mean Gaussian with covariance matrix  $\mathbf{Q}$ .  $L$  is set to be even for ease of illustration.

The time stamp vectors between anchors  $j$  and  $k$  are denoted by the length  $L$  vectors  $\tilde{\mathbf{t}}_{j,k}$  and  $\tilde{\mathbf{r}}_{j,k}$ . They are related to the anchor parameters by

$$(\tilde{\mathbf{t}}_{j,k} - \mathbf{1}_L \beta_j^o)(1 + \alpha_j^o) = (\tilde{\mathbf{r}}_{j,k} - \mathbf{1}_L \beta_k^o)(1 + \alpha_k^o) + \mathbf{1}_L^{\perp} \|\mathbf{a}_j^o - \mathbf{a}_k^o\|/c + \mathbf{1}_L^{\perp} \odot \tilde{\mathbf{n}}_{j,k} \quad (2)$$

where  $j = 1, 2, \dots, M-1, k = j+1, j+2, \dots, M$ . The noise vector  $\tilde{\mathbf{n}} = [\tilde{\mathbf{n}}_{1,2}^T, \tilde{\mathbf{n}}_{1,3}^T, \dots, \tilde{\mathbf{n}}_{j,k}^T, \dots, \tilde{\mathbf{n}}_{M-1,M}^T]^T$  is zero-mean Gaussian with covariance matrix  $\tilde{\mathbf{Q}}$ . We further assume  $\epsilon_{\mathbf{a}}$ ,  $\mathbf{n}$  and  $\tilde{\mathbf{n}}$  are uncorrelated with one another [10, 14, 18, 26].

We next develop an algorithm to jointly estimate  $\theta_b^o$  and  $\theta_{\mathbf{a}}^o$  using (1), (2) and the statistical distribution of anchor uncertainties.

### 3. ALGORITHM

The proposed algorithm employs multi-stage processing by introducing auxiliary variables, using nonlinear transformation and applying weighted least squares (WLS) optimization to obtain the solution. The number of auxiliary variables decreases and the estimation accuracy increases from stage to stage. The algorithm derivation ignores the second and higher order noise terms, which is valid under the small noise condition

$$(C1) \|\epsilon_{\mathbf{a},i}\| \ll \|\mathbf{a}_i^o - \mathbf{b}^o\|, \|\epsilon_{\mathbf{a},j}\| \ll \|\mathbf{a}_j^o - \mathbf{a}_k^o\|, \|\epsilon_{\mathbf{a},k}\| \ll \|\mathbf{a}_j^o - \mathbf{a}_k^o\|$$

for  $i = 1, 2, \dots, M, j = 1, 2, \dots, M-1$  and  $k = j+1, j+2, \dots, M$ . It means the anchor position uncertainty is insignificant relative to the node distances and it is easily satisfied with widely deployed nodes [14, 18]. The algorithm described below is for fully connected network to simplify the presentation and it can be modified directly for partially connected network.

*First Stage:* We begin from (1) and express the anchor parameters in terms of the available noisy values by using

$$\|\mathbf{a}_i^o - \mathbf{b}^o\| = \|\mathbf{a}_i - \epsilon_{\mathbf{a},i} - \mathbf{b}^o\| \simeq \|\mathbf{a}_i - \mathbf{b}^o\| - \rho_i^T \epsilon_{\mathbf{a},i} \quad (3)$$

and

$$\beta_i^o \alpha_i^o = \beta_i \alpha_i^o - \epsilon_{\beta,i} \alpha_i^o, \quad i = 1, 2, \dots, M. \quad (4)$$

(3) is obtained from the Taylor-series expansion up to linear term of  $\epsilon_{\mathbf{a},i}$  that is valid under (C1), and  $\rho_i = (\mathbf{a}_i - \mathbf{b}^o) / \|\mathbf{a}_i - \mathbf{b}^o\|$ . Let  $\omega_b^o = (1 + \alpha_b^o) \beta_b^o$ . We can then express (1) as

$$\mathbf{1}_L^{\perp} \odot \mathbf{n}_i + \mathbf{1}_L \alpha_i^o \epsilon_{\beta,i} = \mathbf{t}_i - \mathbf{r}_i - \mathbf{1}_L^{\perp} \|\mathbf{a}_i - \mathbf{b}^o\|/c + \mathbf{t}_i \alpha_b^o - \mathbf{1}_L \omega_b^o + \mathbf{1}_L^{\perp} \rho_i^T \epsilon_{\mathbf{a},i}/c - (\mathbf{r}_i - \mathbf{1}_L \beta_i) \alpha_i^o + \mathbf{1}_L \beta_i^o. \quad (5)$$

Applying similar steps to (2) gives

$$\begin{aligned} \mathbf{1}_L^{\perp} \odot \tilde{\mathbf{n}}_{j,k} - \mathbf{1}_L \alpha_j^o \epsilon_{\beta,j} + \mathbf{1}_L \alpha_k^o \epsilon_{\beta,k} &= \tilde{\mathbf{t}}_{j,k} - \tilde{\mathbf{r}}_{j,k} \\ &- \mathbf{1}_L^{\perp} \|\mathbf{a}_i - \mathbf{a}_j\|/c + \mathbf{1}_L^{\perp} \rho_{j,k}^T \epsilon_{\mathbf{a},j}/c + (\tilde{\mathbf{t}}_{j,k} - \mathbf{1}_L \beta_j) \alpha_j^o \\ &- \mathbf{1}_L \beta_j^o - \mathbf{1}_L^{\perp} \rho_{j,k}^T \epsilon_{\mathbf{a},k}/c - (\tilde{\mathbf{r}}_{j,k} - \mathbf{1}_L \beta_k) \alpha_k^o + \mathbf{1}_L \beta_k^o \end{aligned} \quad (6)$$

where we have used the approximation  $\|\mathbf{a}_j^o - \mathbf{a}_k^o\| \simeq \|\mathbf{a}_j - \mathbf{a}_k\| - \rho_{j,k}^T \epsilon_{\mathbf{a},j} + \rho_{j,k}^T \epsilon_{\mathbf{a},k}$  from (C1) and  $\rho_{j,k} = (\mathbf{a}_j - \mathbf{a}_k) / \|\mathbf{a}_j - \mathbf{a}_k\|$ .

(5) and (6) are linear with respect to the unknown vector  $\boldsymbol{\varphi}_1^o = [\boldsymbol{\varphi}_b^{oT}, \boldsymbol{\varphi}_{\mathbf{a}}^{oT}]^T$  where  $\boldsymbol{\varphi}_b^o = [\|\mathbf{a}_1 - \mathbf{b}^o\|, \dots, \|\mathbf{a}_M - \mathbf{b}^o\|, \alpha_b^o, \omega_b^o]^T$  and  $\boldsymbol{\varphi}_{\mathbf{a}}^o = [\epsilon_{\mathbf{a},1}^o, \alpha_1^o, \beta_1^o, \dots, \epsilon_{\mathbf{a},M}^o, \alpha_M^o, \beta_M^o]^T$ . Note that we have introduced  $M$  variables  $\|\mathbf{a}_i - \mathbf{b}^o\|, i = 1, 2, \dots, M$ , to represent  $\mathbf{b}^o$  indirectly. In addition, rather than solving  $\mathbf{a}_i^o$  directly, we estimate the correction term  $\epsilon_{\mathbf{a},i}$ .

Left multiplying  $\mathbf{1}_L^{\perp}$  elementwise on the two sides of (5) and (6), stacking (5) for  $i = 1, 2, \dots, M$  and (6) for  $k = j+1, j+2, \dots, M$  first and  $j = 1, 2, \dots, M-1$  next, and using the statistical distribution of  $\epsilon_{\mathbf{a}}$  yield the matrix equation

$$\mathbf{B}_1 \mathbf{e}_1 = \mathbf{h}_1 - \mathbf{G}_1 \boldsymbol{\varphi}_1^o \quad (7)$$

where  $\mathbf{B}_1, \mathbf{e}_1, \mathbf{h}_1$  and  $\mathbf{G}_1$  are defined in Appendix A. The WLS solution of  $\boldsymbol{\varphi}_1^o$  [27] is

$$\boldsymbol{\varphi}_1 = \left( \mathbf{G}_1^T \mathbf{W}_1 \mathbf{G}_1 \right)^{-1} \mathbf{G}_1^T \mathbf{W}_1 \mathbf{h}_1 \quad (8)$$

and the weighting matrix  $\mathbf{W}_1$  is

$$\mathbf{W}_1 = \left( \mathbf{B}_1 \text{diag} \left( \mathbf{Q}, \tilde{\mathbf{Q}}, \mathbf{Q}_{\mathbf{a}} \right) \mathbf{B}_1^T \right)^{-1}. \quad (9)$$

*Second Stage:* The second stage exploits the auxiliary variables  $\|\mathbf{a}_i - \mathbf{b}^o\|$  to improve the estimation accuracy. Let  $\mathbf{e}_2 = \boldsymbol{\varphi}_1 - \boldsymbol{\varphi}_1^o$  be the estimation error of  $\boldsymbol{\varphi}_1$ . From the definition of  $\boldsymbol{\varphi}_1^o$  and  $\omega_b^o = (1 + \alpha_b^o) \beta_b^o$ , for  $i = 1, 2, \dots, M$ ,

$$2\varphi_1^o(i) e_2(i) \simeq \varphi_1^2(i) - \|\mathbf{a}_i\|^2 + 2\mathbf{a}_i^T \mathbf{b}^o - \|\mathbf{b}^o\|^2 \quad (10a)$$

$$e_2(M+1) = \varphi_1(M+1) - \alpha_b^o \quad (10b)$$

$$e_2(M+2) - \beta_b^o e_2(M+1) = \varphi_1(M+2) - (1 + \varphi_1(M+1)) \beta_b^o \quad (10c)$$

where we have neglected  $e_2^2(i)$ . Since the estimation errors within  $\boldsymbol{\varphi}_1^o = [\boldsymbol{\varphi}_b^{oT}, \boldsymbol{\varphi}_{\mathbf{a}}^{oT}]^T$  are correlated, we set  $\boldsymbol{\varphi}_2^o = [\mathbf{b}^{oT}, \|\mathbf{b}^o\|^2, \alpha_b^o, \beta_b^o, \boldsymbol{\varphi}_{\mathbf{a}}^{oT}]^T$  and obtain the matrix equation

$$\mathbf{B}_2 \mathbf{e}_2 = \mathbf{h}_2 - \mathbf{G}_2 \boldsymbol{\varphi}_2^o \quad (11)$$

where  $\mathbf{B}_2, \mathbf{h}_2$  and  $\mathbf{G}_2$  are defined in Appendix A. The WLS solution is

$$\boldsymbol{\varphi}_2 = \left( \mathbf{G}_2^T \mathbf{W}_1 \mathbf{G}_2 \right)^{-1} \mathbf{G}_2^T \mathbf{W}_1 \mathbf{h}_2 \quad (12)$$

where

$$\mathbf{W}_2 = \left( \mathbf{B}_2 \text{cov}(\boldsymbol{\varphi}_1) \mathbf{B}_2^T \right)^{-1} \simeq \mathbf{B}_2^{-T} \mathbf{G}_1^T \mathbf{W}_1 \mathbf{G}_1 \mathbf{B}_2^{-1}. \quad (13)$$

*Third Stage:* We shall represent  $\boldsymbol{\varphi}_2 = \boldsymbol{\varphi}_2^o + \mathbf{e}_3$ . The elements  $\mathbf{b}^o$  and  $\|\mathbf{b}^o\|$  in  $\boldsymbol{\varphi}_2^o$  are related. Since  $\boldsymbol{\varphi}_2^o(1:K) = \mathbf{b}^o$ , we have over the small error region

$$2\boldsymbol{\varphi}_2(1:K) \odot \mathbf{e}_3(1:K) \simeq \boldsymbol{\varphi}_2(1:K) \odot \boldsymbol{\varphi}_2(1:K) - \mathbf{b}^o \odot \mathbf{b}^o. \quad (14)$$

The  $(K+1)$ -th element of  $\boldsymbol{\varphi}_2$  can be expressed as

$$e_3(K+1) = \varphi_2(K+1) - \mathbf{1}_K^T (\mathbf{b}^o \odot \mathbf{b}^o). \quad (15)$$

The unknown vector in this stage is  $\boldsymbol{\varphi}_3^o = \left[ (\mathbf{b}^o \odot \mathbf{b}^o)^T, \alpha_b^o, \beta_b^o, \boldsymbol{\varphi}_a^{oT} \right]^T$ . From (14) and (15) and carrying the other elements of  $\boldsymbol{\varphi}_2^o$  yield

$$\mathbf{B}_3 \mathbf{e}_2 = \mathbf{h}_3 - \mathbf{G}_3 \boldsymbol{\varphi}_3^o \quad (16)$$

whose solution is

$$\boldsymbol{\varphi}_3 = \left( \mathbf{G}_3^T \mathbf{W}_3 \mathbf{G}_3 \right)^{-1} \mathbf{G}_3^T \mathbf{W}_3 \mathbf{h}_3. \quad (17)$$

$\mathbf{B}_3, \mathbf{h}_3, \mathbf{G}_3$  are given in Appendix A and  $\mathbf{W}_3$  is

$$\mathbf{W}_3 = \left( \mathbf{B}_3 \text{cov}(\boldsymbol{\varphi}_2) \mathbf{B}_3^T \right)^{-1} \simeq \mathbf{B}_3^{-T} \mathbf{G}_2^T \mathbf{W}_2 \mathbf{G}_2 \mathbf{B}_3^{-1}. \quad (18)$$

*Fourth Stage:* The last stage maps the elements of  $\boldsymbol{\varphi}_3^o$  back to  $\boldsymbol{\theta}_b^o$  and  $\boldsymbol{\theta}_a^o$ . For the sensor node,

$$\begin{aligned} \mathbf{b} &= \text{diag}(\text{sgn}(\boldsymbol{\varphi}_2(1:K))) \sqrt{\boldsymbol{\varphi}_3(1:K)}, \\ \alpha_b &= \varphi_3(K+1), \beta_b = \varphi_3(K+2). \end{aligned} \quad (19)$$

where  $\text{sgn}$  is the signum function. For the  $i$ -th anchor node,

$$\begin{aligned} \hat{\mathbf{a}}_i &= \mathbf{a}_i - \boldsymbol{\varphi}_3((K+2)i+1:(K+2)i+K), \\ \hat{\alpha}_i &= \varphi_3((K+2)i+K+1), \hat{\beta}_i = \varphi_3((K+2)(i+1)). \end{aligned} \quad (20)$$

The covariance matrix for the  $\boldsymbol{\theta}^o = [\boldsymbol{\theta}_b^{oT}, \boldsymbol{\theta}_a^{oT}]^T$  is [18]

$$\text{cov}(\boldsymbol{\theta}) = \mathbf{B}_4^{-1} \text{cov}(\boldsymbol{\varphi}_3) \mathbf{B}_4^{-T} \simeq \left( \mathbf{B}_4^T \mathbf{G}_3^T \mathbf{W}_3 \mathbf{G}_3 \mathbf{B}_4 \right)^{-1} \quad (21)$$

where  $\mathbf{B}_4 = \text{diag}(\text{diag}(\mathbf{b}^o), \mathbf{I}_2, \mathbf{I}_M \otimes \text{diag}(-\mathbf{I}_K, \mathbf{I}_2))$ .

In summary, the proposed algorithm evaluates (8), (12), (17), (19) and (20) in sequence. The algorithm requires  $M \geq K+1$  to ensure the number of unknowns in the first stage is not less than that of the second stage.

#### 4. ANALYSIS

The CRLB for  $\boldsymbol{\theta}^o$  is given in (23). The analysis uses the small noise condition (C1) as well as those of the followings:

$$(C2) \quad |\epsilon_{\alpha,i}| \ll 1 + \alpha_i^o$$

$$(C3) \quad |\epsilon_{\beta,i}| \ll |r_i(l) - \beta_i^o|, |\epsilon_{\beta,j}| \ll |\tilde{t}_{j,k}(l) - \beta_j^o|, |\epsilon_{\beta,k}| \ll |\tilde{r}_{j,k}(l) - \beta_k^o|$$

$$(C4) \quad |n_i(l)| \ll \|\mathbf{b}^o - \mathbf{a}_i^o\|/c, |\tilde{n}_{j,k}(l)| \ll \|\mathbf{a}_j^o - \mathbf{a}_k^o\|/c$$

for  $i = 1, 2, \dots, M, j = 1, 2, \dots, M-1, k = j+1, j+2, \dots, M$  and  $l = 1, 2, \dots, L$ . These conditions are often satisfied in practice for WSNs [18].

Sequentially substituting  $\mathbf{W}_3$  in (18),  $\mathbf{W}_2$  in (13) and  $\mathbf{W}_1$  in (9) to (21) gives

$$\text{cov}(\boldsymbol{\theta}) = \left( \mathbf{G}_4^T \text{diag}(\mathbf{Q}, \tilde{\mathbf{Q}}, \mathbf{Q}_a) \right)^{-1} \mathbf{G}_4 \quad (22)$$

where  $\mathbf{G}_4 = \mathbf{B}_1^{-1} \mathbf{G}_1 \mathbf{B}_2^{-1} \mathbf{G}_2 \mathbf{B}_3^{-1} \mathbf{G}_3 \mathbf{B}_4$ . Following similar steps in Appendix G of [18], when (C1)–(C4) are satisfied, we can validate that  $\mathbf{G}_4 \simeq \partial(\mathbf{p} - \mathbf{q})/\partial\boldsymbol{\theta}^{oT}$ , where  $\mathbf{p}$  and  $\mathbf{q}$  are defined in Appendix B. Hence the proposed estimator provides the CRLB performance under the small noise conditions.

## 5. SIMULATION

The simulation results presented are the averages from 100 randomly generated geometries. Each geometry consists of 1 sensor and 4 anchor nodes whose positions are created by a uniform random number generator in an area of 40 m  $\times$  40 m with the following constraints to avoid bad configuration: (1)  $\|\mathbf{a}_i^o - \mathbf{a}_j^o\| > 10$  m; (2)  $15^\circ < \arccos(\boldsymbol{\rho}_{i,j}^T \boldsymbol{\rho}_{i,k}) < 165^\circ$ ; where  $i, j, k = 1, 2, \dots, M$  and  $i \neq j \neq k$ . We also impose transmission range limit of 30 m [28] in the nodes to validate the partial connected scenario of the proposed algorithm, although it was presented with full connection in Section 4. The clock drifts  $\alpha_b^o, \alpha_i^o$  and offsets  $\beta_b^o, \beta_i^o, i = 1, 2, \dots, M$ , are randomly sampled from the uniform distributions over  $[-0.002, 0.002]$  and  $[1, 10]$   $\mu\text{s}$  respectively. We set  $\mathbf{Q}_a = \text{diag}(\mathbf{Q}_{a,1}, \dots, \mathbf{Q}_{a,M})$ , where  $\mathbf{Q}_{a,i} = \text{diag}(\sigma_{a,i}^2 \mathbf{I}_2, \sigma_{\alpha,i}^2, \sigma_{\beta,i}^2)$  and  $\sigma_{a,i}, \sigma_{\alpha,i}, \sigma_{\beta,i}$  are randomly drawn over  $[0.1, \sqrt{0.1}]$  m [29],  $[10^{-4}, \sqrt{10^{-7}}]$  [14] and  $[30, 150]$  ns [30] from uniform distribution separately for different anchors. Also,  $\mathbf{Q} = \sigma^2 \mathbf{I}_{ML}$  and  $\tilde{\mathbf{Q}} = \sigma^2 \mathbf{I}_{M(M-1)L/2}$  and  $L = 8$ . The number of ensemble runs in each geometry is 5,000. To the best of our knowledge, we do not find in literature any work solving similar problem for performance comparison.

Fig. 2 shows the estimation accuracy of the sensor and anchor node positions as the time measurement noise power  $\sigma^2$  increases. The proposed algorithm achieves the CRLB accuracy for both anchor and sensor nodes pretty well. When  $\sigma^2$  is small, e.g. 0.1 ns<sup>2</sup>, the anchor position accuracy is improved by nearly 5 dB.

Figs. 3 and 4 give the result of the clock drifts and offsets. The proposed algorithm attains the CRLB as anticipated by the analysis, and it effectively reduces the anchor clock drift and offset uncertainties.

## 6. CONCLUSION

We have developed a closed-form algebraic efficient solution to estimate the positions and clocks of a sensor node and at the same time refine those of the anchors, using two-way message exchanges among the nodes. The proposed algorithm has been shown both analytically and experimentally to reach the CRLB accuracy for Gaussian noise over the small error region. The refined anchor positions and clocks will be able to the localization and synchronization of subsequent sensor nodes in a WSN.

### APPENDIX A. THE MATRICES AND VECTORS IN ALGORITHM DEVELOPMENT

The  $\mathbf{B}_1, \mathbf{e}_1, \mathbf{h}_1$  and  $\mathbf{G}_1$  in (7) are

$$\mathbf{B}_1 = \begin{bmatrix} \mathbf{I}_{M(M+1)L/2} & [\mathbf{B}_b^T, \mathbf{B}_{a,1}^T, \dots, \mathbf{B}_{a,M-1}^T]^T \\ \mathbf{O}_{(K+2)M \times M(M+1)L/2} & \mathbf{I}_M \otimes \text{diag}(-\mathbf{I}_K, \mathbf{I}_2) \end{bmatrix}$$

$$\mathbf{B}_b = \text{diag}(\mathbf{1}_L^T \alpha_1^o, \dots, \mathbf{1}_L^T \alpha_M^o) \otimes [\mathbf{0}_{K+1}^T, 1]$$

$$\mathbf{B}_{a,j} = [\mathbf{B}_{a,j,j+1}^T, \dots, \mathbf{B}_{a,j,M}^T]^T$$

$$\mathbf{B}_{a,j,k} = [\mathbf{0}_{j-1}^T, -\alpha_j^o, \mathbf{0}_{k-j-1}^T, \alpha_k^o, \mathbf{0}_{M-k}^T] \otimes \mathbf{1}_L^T \otimes [\mathbf{0}_{K+1}^T, 1]$$

$$\mathbf{e}_1 = [\mathbf{n}^T, \tilde{\mathbf{n}}^T, \mathbf{e}_a^T]^T, \mathbf{h}_1 = [\mathbf{h}_b^T, \mathbf{h}_{a,1}^T, \dots, \mathbf{h}_{a,M-1}^T, \mathbf{h}_\theta^T]^T$$

$$\mathbf{h}_b = \mathbf{1}_{ML}^T \odot \left[ (\mathbf{t}_1 - \mathbf{r}_1)^T, \dots, (\mathbf{t}_M - \mathbf{r}_M)^T \right]^T$$

$$\mathbf{h}_{a,j} = [\mathbf{h}_{a,j,j+1}^T, \dots, \mathbf{h}_{a,j,M}^T]^T$$

$$\mathbf{h}_{a,j,k} = \mathbf{1}_L^T \odot \left( \tilde{\mathbf{t}}_{j,k} - \tilde{\mathbf{r}}_{j,k} \right) - \mathbf{1}_L \|\mathbf{a}_j - \mathbf{a}_k\|/c$$

$$\mathbf{h}_\theta = [\mathbf{0}_K^T, \alpha_1, \beta_1, \dots, \mathbf{0}_K^T, \alpha_M, \beta_M]^T$$

$$\mathbf{G}_1 = [\mathbf{G}_b^T, \mathbf{G}_{a,1}^T, \dots, \mathbf{G}_{a,M-1}^T, [\mathbf{O}_{(K+2)M \times (2+M)}, \mathbf{I}_{(K+2)M}]^T]^T$$

$$\mathbf{G}_b = [\mathbf{G}_{b,1}^T, \dots, \mathbf{G}_{b,M}^T]^T, \mathbf{G}_{a,j} = [\mathbf{G}_{a,j,j+1}^T, \dots, \mathbf{G}_{a,j,M}^T]^T$$

$$\mathbf{G}_{b,i} = \begin{bmatrix} \mathbf{O}_{L \times (i-1)}, \mathbf{1}_L/c, \mathbf{O}_{L \times (M-i)}, -\mathbf{1}_L^\perp \odot \mathbf{t}_i, \mathbf{1}_L^\perp, \mathbf{O}_{L \times (K+2)(i-1)}, \\ -\mathbf{1}_L \rho_i^T/c, \mathbf{1}_L^\perp \odot \mathbf{r}_i - \mathbf{1}_L^\perp \beta_i, -\mathbf{1}_L^\perp, \mathbf{O}_{L \times (K+2)(M-i)} \end{bmatrix}$$

$$\mathbf{G}_{a,j,k} = \begin{bmatrix} \mathbf{O}_{L \times (M-K+(K+2)j)}, -\mathbf{1}_L \rho_{j,k}^T/c, \mathbf{1}_L^\perp \beta_j - \mathbf{1}_L^\perp \odot \tilde{\mathbf{t}}_{j,k}, \mathbf{1}_L^\perp, \\ \mathbf{O}_{L \times (K+2)(k-j-1)}, \mathbf{1}_L \rho_{j,k}^T/c, \mathbf{1}_L^\perp \odot \tilde{\mathbf{r}}_{j,k} - \mathbf{1}_L^\perp \beta_k, -\mathbf{1}_L^\perp, \\ \mathbf{O}_{L \times (K+2)(M-k)} \end{bmatrix}.$$

The  $\mathbf{B}_2$ ,  $\mathbf{h}_2$  and  $\mathbf{G}_2$  in (11) are

$$\mathbf{B}_2 = \text{diag} \left( 2\varphi_1^o(1), \dots, 2\varphi_1^o(M), \begin{bmatrix} 1 & 0 \\ -\beta_b^o & 1 \end{bmatrix}, \mathbf{I}_{(K+2)M} \right)$$

$$\mathbf{h}_2 = [\varphi_1^2(1) - \|\mathbf{a}_1\|^2, \dots, \varphi_1^2(M) - \|\mathbf{a}_M\|^2, \varphi_1^T(M+1 : (K+3)M+2)]^T$$

$$\mathbf{G}_2 = \text{diag} \left( \begin{bmatrix} -2[\mathbf{a}_1, \dots, \mathbf{a}_M] \\ \mathbf{1}_M^T \end{bmatrix}^T, 1, 1 + \varphi_1(M+1), \mathbf{I}_{(K+2)M} \right).$$

In (16), the  $\mathbf{B}_3$ ,  $\mathbf{h}_3$  and  $\mathbf{G}_3$  are

$$\mathbf{B}_3 = \text{diag} (2\text{diag}(\boldsymbol{\varphi}_2(1:K)), \mathbf{I}_{(K+2)M+3})$$

$$\mathbf{h}_3 = [(\boldsymbol{\varphi}_2(1:K) \odot \boldsymbol{\varphi}_2(1:K))^T, \boldsymbol{\varphi}_2^T(K+1 : (K+2)(M+1)+1)]^T$$

$$\mathbf{G}_3 = \text{diag} (\mathbf{I}_K, \mathbf{1}_K)^T, \mathbf{I}_{2+(K+2)M}.$$

For implementation, the true anchor clock drifts in  $\mathbf{B}_1$  are replaced by their noisy values.  $\beta_b^o$  in  $\mathbf{B}_2$  is replaced by  $\varphi_1(M+2)/(1+\varphi_1(M+1))$ . The other unknown elements in  $\mathbf{B}_2$  are approximated by their estimates from the previous stage. The error introduced by the approximation is negligible [18].

## APPENDIX B. CRLB

Given (1) and (2), the CRLB for  $\theta^o$ , by following similar steps in [14, 18], is

$$\text{CRLB}(\theta^o) = \left( \partial(\mathbf{p} - \mathbf{q})^T / \partial \theta^o \text{diag}(\mathbf{Q}, \tilde{\mathbf{Q}}, \mathbf{Q}_a)^{-1} \partial(\mathbf{p} - \mathbf{q}) / \partial \theta^{oT} \right)^{-1} \quad (23)$$

where  $\mathbf{p} = [\mathbf{p}_{b,1}^T, \dots, \mathbf{p}_{b,M}^T, \mathbf{p}_{a,1}^T, \dots, \mathbf{p}_{a,M-1}^T, \boldsymbol{\theta}_a^T]^T$ ,  $\mathbf{q} = [\mathbf{q}_{b,1}^T, \dots, \mathbf{q}_{b,M}^T, \mathbf{q}_{a,1}^T, \dots, \mathbf{q}_{a,M-1}^T, \boldsymbol{\theta}_a^{oT}]^T$ ,  $\mathbf{p}_{b,i} = \mathbf{1}_L^\perp \odot (\mathbf{t}_i - \mathbf{1}_L \beta_b^o) (1 + \alpha_b^o)$ ,  $\mathbf{q}_{b,i} = \mathbf{1}_L^\perp \odot (\mathbf{r}_i - \mathbf{1}_L \beta_i^o) (1 + \alpha_i^o) + \mathbf{1}_L \|\mathbf{a}_i^o - \mathbf{b}^o\|/c$ ,  $\mathbf{p}_{a,j} = [\mathbf{p}_{a,j,j+1}^T, \dots, \mathbf{p}_{a,j,M}^T]^T$ ,  $\mathbf{p}_{a,j,k} = \mathbf{1}_L^\perp \odot (\tilde{\mathbf{t}}_{j,k} - \mathbf{1}_L \beta_j^o) (1 + \alpha_j^o)$ ,  $\mathbf{q}_{a,j} = [\mathbf{q}_{a,j,j+1}^T, \dots, \mathbf{q}_{a,j,M}^T]^T$ ,  $\mathbf{q}_{a,j,k} = \mathbf{1}_L^\perp \odot (\tilde{\mathbf{r}}_{j,k} - \mathbf{1}_L \beta_k^o) (1 + \alpha_k^o) + \mathbf{1}_L \|\mathbf{a}_j^o - \mathbf{a}_k^o\|/c$ ,  $i = 1, 2, \dots, M$ ,  $j = 1, 2, \dots, M-1$  and  $k = j+1, j+2, \dots, M$ . The differentiation can be computed following similar steps in Appendix F of [18] and is omitted here for brevity.

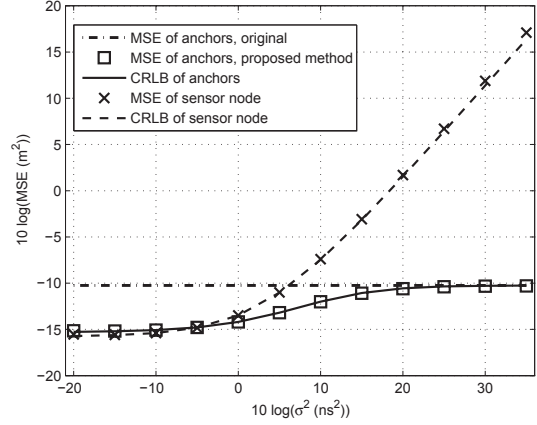


Fig. 2. Position estimation performance of the sensor node and anchors under different time measurement noise powers.

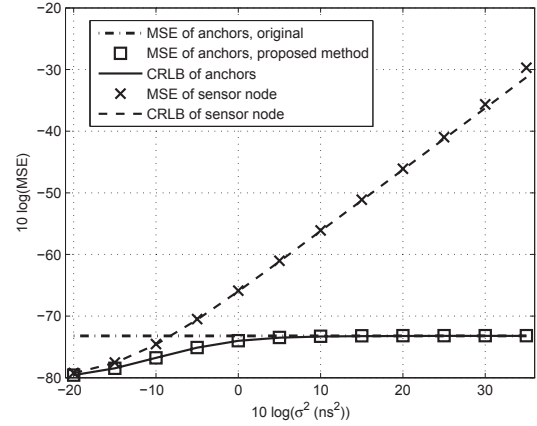


Fig. 3. Estimation accuracy of clock drifts of the sensor node and anchors under different time measurement noise powers.

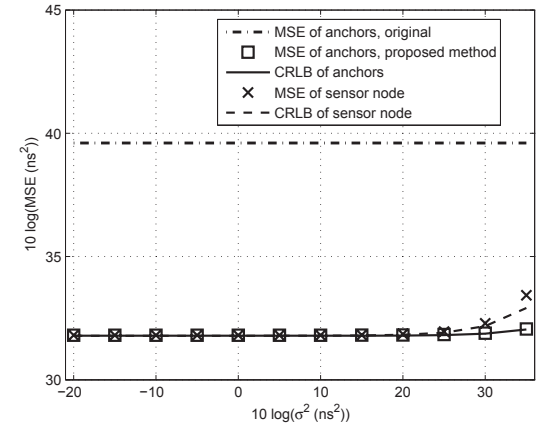


Fig. 4. Estimation accuracy of clock offsets of the sensor node and anchors under different time measurement noise powers.

## 7. REFERENCES

- [1] M. R. Gholami, L. Tetrashvili, E. G. Strom, and Y. Censor, "Cooperative wireless sensor network positioning via implicit convex feasibility," *IEEE Trans. Signal Process.*, vol. 61, no. 23, pp. 5830-5840, Dec. 2013.
- [2] A. Simonetto and G. Leus, "Distributed maximum likelihood sensor network localization," *IEEE Trans. Signal Process.*, vol. 62, no. 6, pp. 1424-1437, Mar. 2014.
- [3] G. Wang, H. Chen, Y. Li, and N. Ansari, "NLOS error mitigation for TOA-based localization via convex relaxation," *IEEE Trans. Wireless Commun.*, vol. 13, no. 8, pp. 4119-4131, Aug. 2014.
- [4] K. C. Ho, "Bias reduction for an explicit solution of source localization using TDOA," *IEEE Trans. Signal Process.*, vol. 60, no. 5, pp. 2101-2114, May 2012.
- [5] S. Kay and N. Vankayalapati, "Improvement of TDOA position fixing using the likelihood curvature," *IEEE Trans. Signal Process.*, vol. 61, no. 8, pp. 1910-1914, Apr. 2013.
- [6] Y. T. Chan and K. C. Ho, "A simple and efficient estimator for hyperbolic location," *IEEE Trans. Signal Process.*, vol. 42, no. 8, pp. 1905-1915, Aug. 1994.
- [7] G. Wang and H. Chen, "An importance sampling method for TDOA-based source localization," *IEEE Trans. Wireless Commun.*, vol. 10, no. 5, pp. 1560-1568, May 2011.
- [8] J. Elson, L. Girod, and D. Estrin, "Fine-grained network time synchronization using reference broadcasts," in *Proc. Symp. Operating Syst. Design Implementation*, Boston, MA, Dec. 2002, pp. 147-163.
- [9] M. Maroti, B. Kusy, G. Simon, and A. Ledeczi, "The flooding time synchronization protocol," in *Proc. SenSys 04*, Baltimore, MD, Nov. 2004, pp. 39-49.
- [10] B. Etzlinger, H. Wymeersch, and A. Springer, "Cooperative synchronization in wireless networks," *IEEE Trans. Signal Process.*, vol. 62, no. 11, pp. 2837-2849, Jun. 2014.
- [11] J. Zheng and Y.-C. Wu, "Localization and time synchronization in wireless sensor networks: A unified approach," in *Proc. IEEE Asia Pacific Conf. on Circuits and Sys.*, Macao, China, Nov.-Dec. 2008, pp. 594-597.
- [12] S. Zhu and Z. Ding, "Joint synchronization and localization using TOAs: A linearization based WLS solution," *IEEE J. Sel. Areas Commun.*, vol. 28, no. 7, pp. 1017-1025, Aug. 2010.
- [13] V. Y. Zhang and A. K. Wong, "Closed-form solution for joint localization and time synchronization in wireless sensor networks," in *Proc. IEEE ICC*, Cape Town, South Africa, May 2010, pp. 1-5.
- [14] J. Zheng and Y.-C. Wu, "Joint time synchronization and localization of an unknown node in wireless sensor networks," *IEEE Trans. Signal Process.*, vol. 58, no. 3, pp. 1309-1320, Mar. 2011.
- [15] Z. Ma and K. C. Ho, "TOA localization in the presence of random sensor position errors," in *Proc. IEEE Int. Conf. Acoust., Speech, Signal Process.*, Prague, Czech Republic, May 2011, pp. 2468-2471.
- [16] Y. Cheng, X. Wang, T. Caelli, X. Li, and B. Moran, "Optimal nonlinear estimation for localization of wireless sensor networks," *IEEE Trans. Signal Process.*, vol. 59, no. 12, pp. 5674-5685, Dec. 2011.
- [17] Y. Wang and K. C. Ho, "TDOA source localization in the presence of synchronization clock bias and sensor position errors," *IEEE Trans. Signal Process.*, vol. 61, no. 18, pp. 4532-4544, Sep. 2013.
- [18] L. Rui and K. C. Ho, "Algebraic solution for joint localization and synchronization of multiple sensor nodes in the presence of beacon uncertainties," *IEEE Trans. Wireless Commun.*, vol. 13, no. 9, pp. 5196-5210, Sep. 2014.
- [19] M. Sun, L. Yang, and K. C. Ho, "Efficient joint source and sensor localization in closed-form," *IEEE Signal Process. Lett.*, vol. 19, pp. 399-402, Jul. 2012.
- [20] M. Sun, Z. Ma, and K. C. Ho, "Joint source localization and sensor position refinement for sensor networks," in *Proc. IEEE Int. Conf. Acoust., Speech, Signal Process.*, Vancouver, Canada, May 2013, pp. 4026-4030.
- [21] O. Jean and A. J. Weiss, "Passive localization and synchronization using arbitrary signals," *IEEE Trans. Signal Process.*, vol. 62, no. 8, pp. 2143-2150, Apr. 2014.
- [22] I. Skog and P. Handel, "Synchronization by two-way message exchanges: Cramer-Rao bounds, approximate maximum likelihood, and offshore submarine positioning," *IEEE Trans. Signal Process.*, vol. 58, no. 4, pp. 2351-2362, Apr. 2010.
- [23] M. Leng and Y. Wu, "Distributed clock synchronization for wireless sensor networks using belief propagation," *IEEE Trans. Signal Process.*, vol. 59, no. 11, pp. 5404-5414, Apr. 2011.
- [24] A. Ahmad, E. Serpedin, H. Nounou, and M. Nounou, "Joint node localization and time-varying clock synchronization in wireless sensor networks," *IEEE Trans. Wireless Commun.*, vol. 12, no. 10, pp. 5322-5333, Oct. 2013.
- [25] Y.-C. Wu, Q. Chaudhari, and E. Serpedin, "Clock synchronization of wireless sensor networks," *IEEE Signal Process. Mag.*, vol. 28, no. 1, pp. 124-138, Jan. 2011.
- [26] J. Kim, J. Lee, E. Serpedin, and K. Qaraqe, "Robust clock synchronization in wireless sensor networks through noise density estimation," *IEEE Trans. Signal Process.*, vol. 59, no. 7, pp. 3035-3047, Jul. 2010.
- [27] S. M. Kay, *Fundamentals of Statistical Signal Process., Estimation Theory*. Englewood Cliffs, NJ: Prentice-Hall, 1993.
- [28] Q. Zou, A. Tarighat, and A. H. Sayed, "Performance analysis and range improvement in multiband-OFDM UWB communications," in *Proc. IEEE Int. Conf. Acoust., Speech, Signal Process.*, Toulouse, France, May 2006, pp. 629-632.
- [29] J. Farrell, T. Givargis, and M. Barth, "Real-time differential carrier phase GPS-aided INS," *IEEE Trans. Contr. Syst. Technol.*, vol. 8, pp. 709-721, Jul. 2000.
- [30] J. Mannermaa, K. Kalliomaki, T. Mansten, and S. Turunen, "Timing performance of various GPS receivers," in *Proc. IEEE Int. Frequency Contr. Symp.*, Besancon, France, Apr. 1999, pp. 287-290.